Exp Brain Res (2007) 180:303–319
DOI 10.1007/s00221-007-0859-6

RESEARCH ARTICLE

Behavioral dynamics of intercepting a moving target

Brett R. Fajen · William H. Warren

Received: 25 January 2006 / Accepted: 5 January 2007 / Published online: 2 February 2007

Abstract From matters of survival like chasing prey, to games like football, the problem of intercepting a target that moves in the horizontal plane is ubiquitous in human and animal locomotion. Recent data show that walking humans turn onto a straight path that leads a moving target by a constant angle, with some transients in the target-heading angle. We test four control strategies against the human data: (1) *pursuit*, or nulling the target-heading angle β, (2) *computing* the required interception angle $\dot{\beta}$, (3) *constant target-heading angle*, or nulling change in the target-heading angle $\dot{\beta}$, and (4) *constant bearing*, or nulling change in the bearing direction of the target $\dot{\psi}$, which is equivalent to nulling change in the target-heading angle while factoring out the turning rate $(\dot{\beta} - \dot{\phi})$. We show that human interception behavior is best accounted for by the constant bearing model, and that it is robust to noise in its input and parameters. The models are also evaluated for their performance with stationary targets, and implications for the informational basis and neural substrate of steering control are considered. The results extend a dynamical systems model of human locomotor behavior from static to changing environments.

B. R. Fajen (✉)
Department of Cognitive Science,
Rensselaer Polytechnic Institute, Carnegie Building 308,
110 8th Street, Troy, NY 12180-3590, USA
e-mail: fajenb@rpi.edu

W. H. Warren
Department of Cognitive and Linguistic Sciences,
Brown University, Providence, USA

Keywords Interception · Visual control · Locomotion · Dynamical systems modeling

Introduction

As we walk about the world each day, our locomotor behavior is effortlessly coordinated with a complex, dynamic environment. Consider, as an extreme example, the American game of football, in which a player must run toward stationary goals, avoid stationary and moving obstacles, intercept and tackle moving targets, and evade pursuit. Similar challenges are faced on a daily basis by animals in the wild, people walking through public spaces, and increasingly by autonomous mobile robots. In order to understand these fundamental abilities, we seek to model the *behavioral dynamics* of locomotion—the time-evolution of behavior as an agent interacts with its environment.

Our approach to this problem begins by modeling a set of elementary locomotor behaviors as simple dynamical systems, including steering to a stationary goal, avoiding a stationary obstacle, intercepting a moving target, and avoiding a moving obstacle. Inspired by the work of Schöner et al. (1995) on robotic control, we recently developed a model of human steering and obstacle avoidance in static environments that generates the time-course of heading direction (Fajen and Warren 2003). One component of the model accurately simulates the paths people take when walking to a stationary goal, while a second component reproduces human detours around an obstacle and predicts routes through novel configurations of obstacles. In the present study, we seek to extend the model to the case of intercepting a moving target. Specifically,

we evaluate four possible control strategies for target interception: (1) *pursuit*, (2) *computing* the required interception angle, (3) *constant target-heading angle*, and (4) *constant bearing*, and test these hypotheses against our empirical data (Fajen and Warren 2004).

Our analysis also bears on the perceptual information used to guide locomotion. It is well established that humans can perceive their direction of heading from optic flow with an accuracy of about 1° under a variety of environmental and self-motion conditions (see Warren 2004, for a review). People can also judge their direction of walking based on proprioceptive and motor information about the locomotor axis, but are an order of magnitude less accurate (Telford et al. 1995; see Israël and Warren 2005, for a review). Thus, walking to a stationary target might be based on several possible variables, including *optic flow*, such that one aligns the heading specified by optic flow with the visual target (Gibson 1950; Warren et al. 2001); *egocentric direction*, such that one aligns the locomotor axis with the egocentric direction of the target (Rushton et al. 1998); *centering*, such that one fixates the target and aligns the body midline with direction of gaze on the basis of proprioception[1](Hollands et al. 2002); or *target drift*, such that one cancels the motion of the target in the field of view, which is equivalent to nulling change in the target-heading angle[2] (Llewellyn 1971; Rushton et al. 2002; Wilkie and Wann 2003, 2005).

In the case of steering to a stationary goal, the evidence indicates that participants rely on both optic flow and egocentric direction. Optic flow tends to dominate when there is sufficient visual surface structure in the scene (Harris and Carré 2001; Li and Warren 2002; Turano et al. 2005; Warren et al. 2001; Wilkie and Wann 2002, 2003; Wood et al. 2000), whereas egocentric direction dominates when visual structure is reduced (Rushton et al. 1998; Harris and Bonas 2002). But paradoxically, in the case of intercepting a moving target, Fajen and Warren (2004; see also Chardenon et al. 2004) found no influence of optic flow and concluded that participants relied solely on the egocentric direction of the target. This inconsistency might be resolved if it turned out that there are different underlying control strategies for stationary and moving targets. Indeed, the present findings suggest that steering to a stationary goal is based on the nulling the target-heading angle, whereas intercepting a moving target is based on nulling change in the direction of the target in space.

Information about self-motion appears to be extracted by cortical networks in the dorsal pathway that integrate multisensory signals and perform sensorimotor transformations related to locomotor control (Duffy 2005; Raffi and Siegel 2004). Single-unit recordings in macaque indicate that cells in area MSTd are selective for large-field optic flow patterns and integrate eye pursuit and vestibular signals; neurons in area VIP have a heading tuning that is invariant over eye movements (Zhang et al. 2004) and integrate tactile and vestibular signals; area 7a cells are sensitive to the pattern and speed of optic flow and exhibit eye position tuning; area STPa neurons respond to both optic flow and object boundaries, and may be sensitive to object-relative heading; flow-sensitive cells in area PEc project to premotor cortex; and even motor cortical neurons in M1 are selective for expansion patterns. Functional neuroimaging studies indicate flow-specific activity in homologous regions of the human brain, including the hMT+ complex (primate MT–MST), VIP, DISPM/L (primate 7a), and STG (primate STP) (Morrone et al. 2000; Peuskens et al. 2001; Vaina and Soloviev 2004). In particular, area STG is activated by heading with respect to landmarks (Vaina and Soloviev 2004), and a region in the superior parietal lobule (SPL) that includes LIP responds to heading errors relative to a roadway in an active steering task (Field et al. 2006). Taken together, these findings suggest a neural substrate for the extraction of target-heading angle and for transformations relevant to the control of steering. A functional model of locomotor control would offer candidate hypotheses about these sensorimotor mappings whose neural implementation could then be investigated.

In what follows, we briefly describe the steering dynamics model for a stationary goal (Fajen and Warren 2003), and then extend the model to the case of intercepting a moving target. We then compare simulations of each control strategy against our previous human data on target interception.

Steering to a stationary goal

We define *heading* (ϕ) as the direction of locomotion with respect to an allocentric reference axis,[3] and

[1] This assumes that the midline is coincident with the locomotor axis, but exceptions include a ''crabbing'' gait for terrestrial animals, a crosswind for aerial animals, and a crosscurrent for aquatic animals.

[2] This assumes that the observer is not rotating. It follows from the basic law of optic flow (Nakayama and Loomis 1974) that the target's angular velocity is proportional to the sine of the target-heading angle and inversely proportional to distance.

[3] The use of an allocentric reference axis to define heading is for convenience of analysis. The perceptual input to the agent is the target-heading angle $\beta = \phi - \psi_m$.

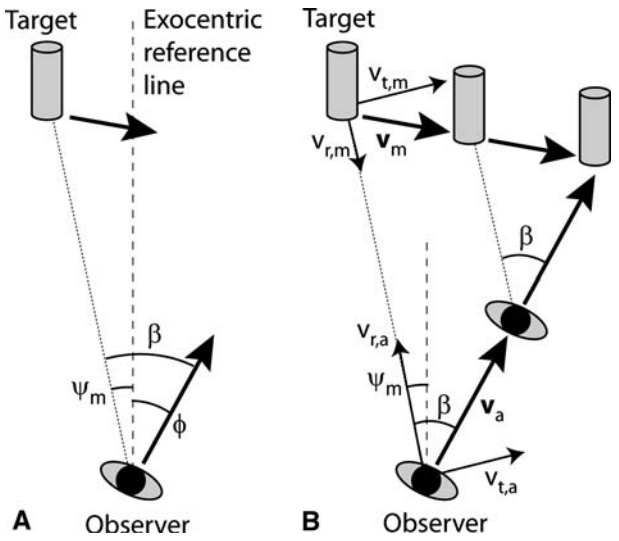

Fig. 1 **a** Definition of variables for the model. **b** Intercepting a moving target will be successful if the agent (i) matches the transverse speed of the target, so $v_{t,a} = v_{t,m}$, and (ii) approaches the target, so $v_{r,a} > v_{r,m}$. The resulting path has a constant target-heading angle β and a constant bearing direction ψ_m

bearing (ψ_g) as the direction of a target with respect to the same axis, at a distance d_g (see Fig. 1a; the subscript g designates that the target is a stationary goal). The *target-heading angle* ($\beta = \phi - \psi_g$) is the difference between the two. To turn onto a straight path toward the goal, the agent must null this heading error and stabilize the heading in the direction of the goal, such that the target-heading angle ($\beta = \phi - \psi_g$) and the turning rate ($\dot{\phi}$) both go to zero before the goal is reached. There is thus an *attractor* of heading at $(\phi, \dot{\phi}) = (\psi_g, 0)$.

The model consists of a system of differential equations that generates a trajectory through the state space $(\phi, \dot{\phi})$—that is, a sequence of headings and turning rates—for a given speed of travel (Fajen and Warren 2003; Fajen et al. 2003). To produce the requisite turns toward the goal, imagine that the heading direction is attached to the goal direction by a damped spring. Analogously, the model describes the angular acceleration of heading as a function of the current goal direction (ψ_g),

$$\ddot{\phi} = -b\dot{\phi} - k_g(\phi - \psi_g)(e^{-c_1 d_g} + c_2) \quad (1)$$

where b, k_g, c_1, and c_2 are parameters. As the agent moves through the environment to the next (x, z) position, the goal angle and distance change, and the next heading and turning rate are determined from Eq. 1. The ''damping'' term $-b\dot{\phi}$ acts as a frictional force that resists turning and is proportional to the turning rate, which tends to keep the path straight and prevents the heading from oscillating about the goal; parameter b expresses the ratio of damping to the body's moment of inertia, in units of s^{-1}. The ''stiffness'' term k_g $(\phi - \psi_g)$ reflects the empirical finding that angular acceleration increases linearly with the target-heading angle over some range (for humans, Fajen and Warren 2003, as well as flies, Reichardt and Poggio 1976); parameter k_g expresses the ratio of stiffness to moment of inertia, in units of s^{-2}. The stiffness is modulated by the distance of the goal, reflecting the finding that turning acceleration increases exponentially with nearer goals $(e^{-c_1 d_g} + c_2)$ (Fajen and Warren 2003). The constant c_1 determines the decay rate with distance in units of m^{-1}, and c_2 determines a minimum value so acceleration does not go to zero at large distances, and is dimensionless. The model fits the mean human time series of target-heading angle for a stationary goal extremely well, with a mean $r^2 = 0.98$ for parameter values of $b = 3.25$, $k_g = 7.50$, $c_1 = 0.40$, and $c_2 = 0.40$ across all conditions.

A second component of the model accurately describes obstacle avoidance by defining a similar spring force that repels the heading away from the direction of a stationary obstacle (Fajen and Warren 2003; Fink et al. in press). A similar distance term is needed because humans turn to avoid near obstacles before they respond to more distant obstacles or goals. The direction of travel is thus determined by the net resultant of all forces acting on the agent at any moment. A route through a complex scene unfolds as the agent tracks the local heading attractor, whose location is determined by the sum of the goal and obstacle components. Our modeling strategy is to fix the parameter values for each component using a basic data set, and then use the model to predict human paths with novel configurations of objects.

We should point out that the goal component (Eq. 1) is a dynamical system that corresponds to a standard proportional-derivative controller, but with a nonlinear stiffness term that depends on distance, whereas the obstacle component is a dynamical system that does not correspond to a PD controller. The pertinent psychological question is what variables are regulated by this relatively simple system to achieve adaptive locomotor behavior.

Strategies for intercepting a moving target

There are a number of ways the steering dynamics model might be extended to account for human paths to a moving target, in the case of a constant velocity target on the ground plane. In this section, we introduce four

possible control strategies and the existing experimental evidence, then go on to formalize and test these hypotheses using the model framework.

Pursuit strategy

One solution for reaching a moving target is to travel directly toward it, bringing the target-heading angle to zero ($\beta = \phi - \psi_m = 0$, where subscript m designates that the target is moving). Under this *pursuit strategy*, the agent would continually turn to track a moving target while traveling forward, yielding a continuously curved path of locomotion. Consistent with this strategy, Rushton et al. (1998) reported that humans walked directly toward a moving target in the open field, tracing out a curved path. However, the target speed was very slow (about 1°/s at the beginning of a trial) and likely insufficient to induce interception. Data from Lenoir et al. (2002) suggest that interception adjustments occur only when the change in the bearing direction reaches 3–5°/s. With faster targets in the open field, we recently found that humans do not walk directly toward the target but turn onto a straight path that leads the target and successfully intercepts it (Fajen and Warren 2004).

Interception strategies

Thus, another solution is to adopt a straight interception path to the target, as illustrated in Fig. 1b. Suppose the agent locomotes with velocity v_a and the target moves with velocity v_m, each having a transverse component perpendicular to the line of sight (subscript t) and a radial component along the line of sight (subscript r). The agent will successfully intercept the target if the following two conditions are satisfied. First, the agent's transverse speed must match the transverse speed of the target ($v_{t,a} = v_{t,m}$). They thus share a common moving reference frame, reducing the problem to 1D. Second, the agent's radial speed must exceed the target's radial speed ($v_{r,a} > v_{r,m}$)[4], so that the distance to the target decreases. These two conditions produce a straight path with a constant bearing direction (ψ_m) as well as a constant *interception angle* ($\hat{\beta}$), that is, a target-heading angle that will intercept the target,

$$\hat{\beta} = \sin^{-1}\left(\frac{v_{t,m}}{v_a}\right) \tag{2}$$

which depends on transverse target speed $v_{t,m}$ and walking speed v_a. Thus, a faster target demands a larger interception angle and/or a faster walking speed, and if target velocity changes, the agent can still intercept the target by adjusting walking speed and/or direction until $v_{t,a} = v_{t,m}$. How, then might an effective interception angle be determined by a locomoting agent? This analysis suggests several possible control strategies.

First, according to a rule of thumb familiar to sailors and pilots, if another craft remains at a constant compass bearing, one is on a collision course and evasive action is called for. This observation suggests an efficient interception strategy: steer so that the bearing direction (ψ_m) remains constant (Chapman 1968). If the target is traveling at a constant velocity, this strategy will yield the shortest straight interception path for a given speed of locomotion. However, maintaining the target's bearing direction requires either a visible external reference frame such as a fixed background or distant landmark, or some other means of compensating for body rotation. Interestingly, dragonflies intercept prey overhead by maintaining a constant angle between the target and the horizon (Olberg et al. 2000). This is equivalent to the constant bearing strategy, using the horizon as a fixed visual reference.

A closely related strategy is to steer so that the target-heading angle (β) remains constant (Chardenon et al. 2002, 2004, 2005; Cutting et al. 1995; Rushton et al. 2002). However, for given initial conditions, there is only one constant angle ($\hat{\beta}$) that will intercept the target on a straight path, while other angles yield spiral paths that lead or lag the target. Thus, a unique interception angle must somehow be determined.

Finally, a third interception strategy is to perceive the distal velocity of the target, as well as one's own speed, and compute the required interception angle ($\hat{\beta}$) that will yield a straight path ahead of the target, according to Eq. 2. However, this approach requires highly accurate perception of object velocities in three-space.

The human evidence is consistent with some type of interception strategy rather than a pursuit strategy. Participants riding down a track (Lenoir et al. 1999a, 2002) or walking on a treadmill (Chardenon et al. 2002, 2004, 2005) adjust their speed to keep the bearing angle and target-heading angle (which are equivalent in this case) approximately constant. However, in those experiments participants could only vary their speed, not their direction of travel, and consequently the constant bearing and constant target-heading angle strategies could not be distinguished. Fajen and Warren (2004) tested the general case of interception in the

[4] We assume that v_r is positive in the direction extending from the agent to the target, such that $v_{r,a} > 0$ and $v_{r,m} < 0$ in Fig. 1b

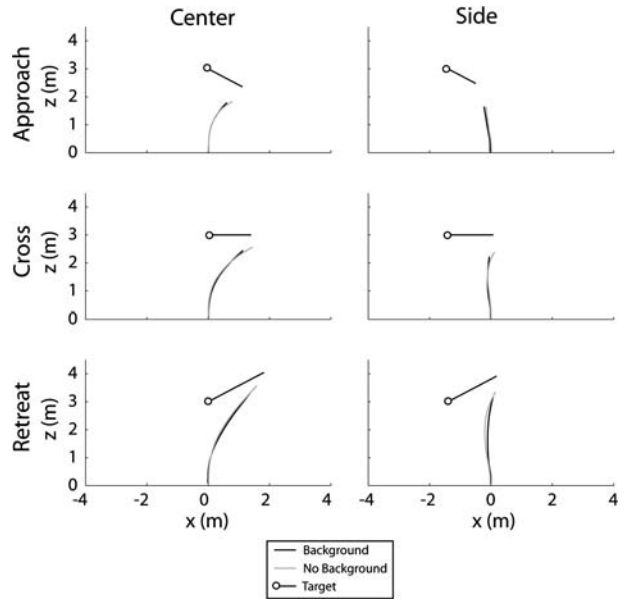

Fig. 2 Mean paths of human subjects intercepting a moving target in each test condition (from Fajen and Warren 2004). *Black lines* represent conditions with a visible Background, *gray lines* the No Background condition. In the Center condition, the target appeared directly ahead on the participant's path, in the Side condition it appeared 25° to the left or right (collapsed). Approach, cross, and retreat indicate the target trajectory, at 0.6 m/s

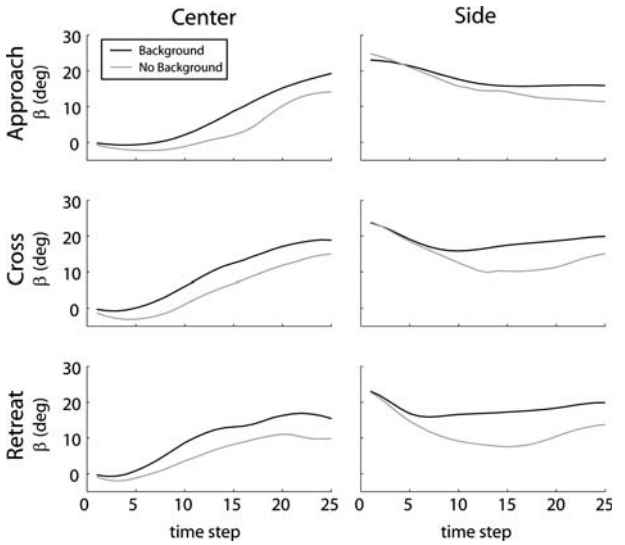

Fig. 3 Mean time series of target-heading angle (β) from Fajen and Warren (2004). *Black lines* represent the Background condition, *gray lines* the No Background condition. Individual trials were normalized to a length of 25 time steps before computing condition means

open field by presenting moving targets to people walking freely in a large virtual environment. The target appeared at a distance of 3 m in depth, either directly ahead of a walking subject or 20° to one side, and moved horizontally on one of three trajectories at a speed of 0.6 m/s (Figs. 2, 3). Participants successfully intercepted the target by leading it for most of the approach (Fig. 2) and walking at a fairly constant speed. However, there were transients in the target-heading angle (Fig. 3), such that participants gradually turned onto a straight path close to the interception angle predicted by Eq. 2. Thus, the dynamics of actual walking behavior depart from an idealized interception strategy. Here, we show that the observed behavior can be best accounted for by casting the constant bearing strategy into the context of a dynamical model of locomotion.

Simulations

We are now ready to formalize the four hypotheses and test them by comparing model simulations against Fajen and Warren's (2004) human data. The methods used in human experiments and model simulations are described in Appendix.

Model #1: Pursuit strategy (null β)

The simplest approach would be to apply Fajen and Warren's (2003) original stationary-target model (Eq. 1) to the case of a moving target. This component acts to bring the heading error with the target to zero ($\beta = \phi - \psi_m = 0$), which amounts to an implementation of the pursuit strategy. However, Fajen and Warren's (2004) data for moving targets suggest that human behavior is inconsistent with a pursuit strategy. To illustrate how the behavior of this null β model differs from the behavior of humans intercepting moving targets, we simulated Eq. 1 and compared the simulations to the data from Fajen and Warren (2004) under the same initial conditions.

We first compared the model paths with the mean human paths (see Fig. 4). It is apparent that the stationary goal model generates continuously curved pursuit paths, rather than turning onto an interception path like the human subjects. The time series of the target-heading angle (β) for the mean human data and the model appear in Fig. 5. Whereas human participants bring the target-heading angle to a leading interception angle close to 20°, the model brings this angle close to zero. In fact, target-heading angle often falls below zero because damping prevents the agent from turning quickly enough to track the moving target. The parameter values used for these simulations were $b = 5.0\ \mathrm{s}^{-1}$, $k_m = 25.0\ \mathrm{s}^{-2}$, $c_1 = 0.40\ \mathrm{m}^{-1}$, and $c_2 = 0.40$, which differ slightly from the original values

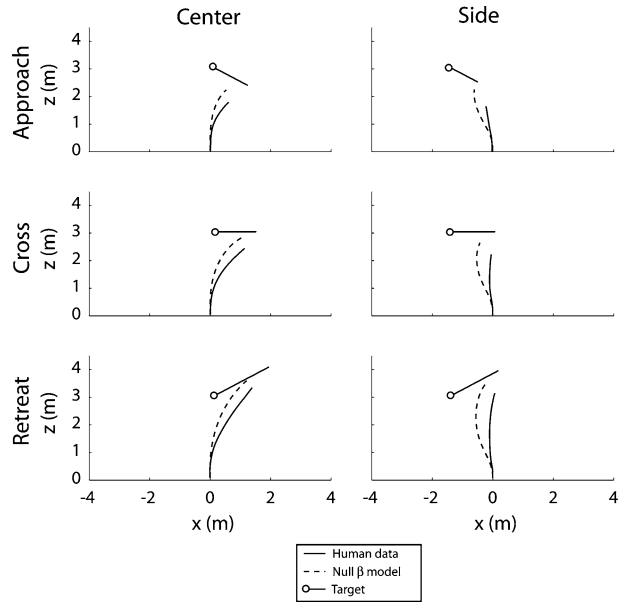

Fig. 4 Model #1: Paths produced by nulling β (*dotted lines*) compared to human data (*solid lines*)

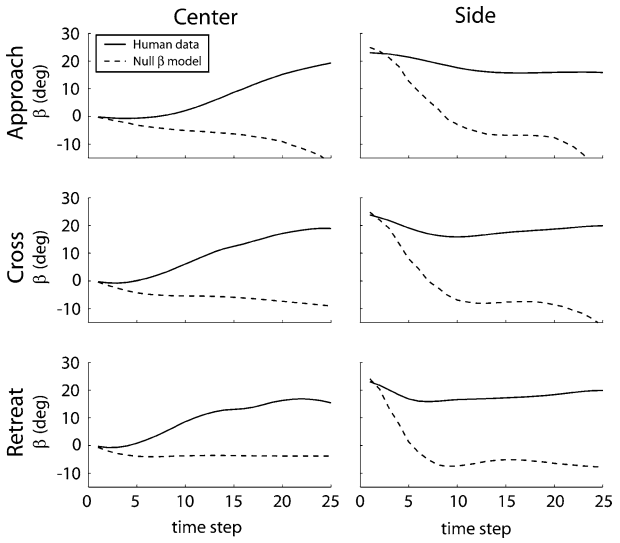

Fig. 5 Model #1: Time series of target-heading angle (β) produced by nulling β (*dotted lines*) compared to human data (*solid lines*)

that best fit the data from Fajen and Warren (2003). When the original parameters were used, the target-heading angle failed to stabilize near zero, and in some cases the agent's path looped around behind the target, so it was necessary to increase both damping (b) and stiffness (k_m). The present parameter values were arrived at by making small changes to the original values until the target-heading angle stabilized near zero. Even with the change in parameters, however, the stationary target component fails to capture human interception behavior.

Model #2: Required interception angle (compute $\hat{\beta}$)

One solution to the problem with Model #1 is to compute the required interception angle ($\hat{\beta}$) as in Eq. 2, and then null the difference between the current target-heading angle β and the required angle $\hat{\beta}$:

$$\ddot{\phi} = -b\dot{\phi} - k_m(\beta - \hat{\beta})(e^{-c_1 d_m} + c_2) \quad (3)$$

This model captures the human behavior well, for the time series of target-heading angle have an rmse = 2.26° and $r^2 = 0.85$. The parameters ($b = 7.0$ s^{-1}, $k_m = 8.0$ s^{-2}, $c_1 = 0.1$ m^{-1}, and $c_2 = 0.5$) were arrived at by fitting the model to the mean target-heading angle time series in each condition, using a least squares procedure that minimized the error in β at every time step (see methods below). The model also has the advantage that it applies to both stationary and moving targets, because $\hat{\beta} = 0$ when the target is not moving, so Eq. 3 reduces to Eq. 1. However, it requires that the interception angle be explicitly computed according to Eq. 2, which presumes that the distal target velocity $v_{t,m}$ and walking speed v_a can be accurately perceived. Furthermore, the model is not robust, for a 10% error in perceived $v_{t,m}$ and v_a at a typical walking speed (1 m/s) can produce as much as a 50% error in the computed interception angle. The $\hat{\beta}$ model thus does not appear to be a viable strategy.

Model #3: Constant target-heading angle (null $\dot{\beta}$)

A third possibility is to arrive at a constant target-heading angle by nulling the change in this angle ($\dot{\beta}$), rather than computing it explicitly. We thus derived an interception component from Eq. 1 by substituting $\dot{\beta} = \dot{\phi} - \dot{\psi}_m$ in place of $\beta = \phi - \psi_g$, so that the model nulls $\dot{\beta}$ instead of β:

$$\begin{aligned}\ddot{\phi} &= -b\dot{\phi} - k_m(\dot{\phi} - \dot{\psi}_m)(d_m + c_1) \\ &= -b\dot{\phi} - k_m\dot{\beta}(d_m + c_1). \end{aligned} \quad (4)$$

The effect of the distance term in Eq. 4 (i.e., $d_m + c_1$) is to increase the influence of the moving target as target distance increases. Without the distance term, the agent makes sluggish turns toward distant targets because $\dot{\beta}$ decreases to zero as distance goes to infinity. The distance term in Eq. 4 effectively offsets this bias by weighting the influence of $\dot{\beta}$ more heavily when the target is further away. The parameter c_1 was included to prevent the influence of the target from dropping to zero as distance decreases. In the simulations reported

below, c_1 was set to 1.0 by default so that the stiffness component never dropped below $k_m(\dot{\phi} - \dot{\psi}_m)$. Thus, c_1 should not be considered an additional free parameter.

The problem with the null-$\dot{\beta}$ model is that it is under-constrained. $\dot{\beta}$ is a function of both the relative motion between the agent and the target (which affects $\dot{\psi}_m$) and the agent's turning rate ($\dot{\phi}$; see Fig 1b). This means that there are two distinct ways to null $\dot{\beta}$ and maintain a constant target-heading angle: the "lead" solution and the "lag" solution. Figure 6a shows an agent nulling $\dot{\beta}$ by turning onto a straight path that leads the target, such that $\dot{\phi} = \dot{\psi}_m = 0$ and $\beta > 0$. Figure 6b shows an agent nulling $\dot{\beta}$ by lagging behind the target while turning at the same rate that the bearing direction of the target is changing, such that $\dot{\phi} = \dot{\psi}_m > 0$ and $\beta < 0$. This yields a continuously curved path that chases the target. The data from Fajen and Warren (2004) indicate that humans always adopt the lead solution. The null $\dot{\beta}$ model, on the other hand, produces the lead solution under some initial conditions, and the lag solution under others. This is illustrated in

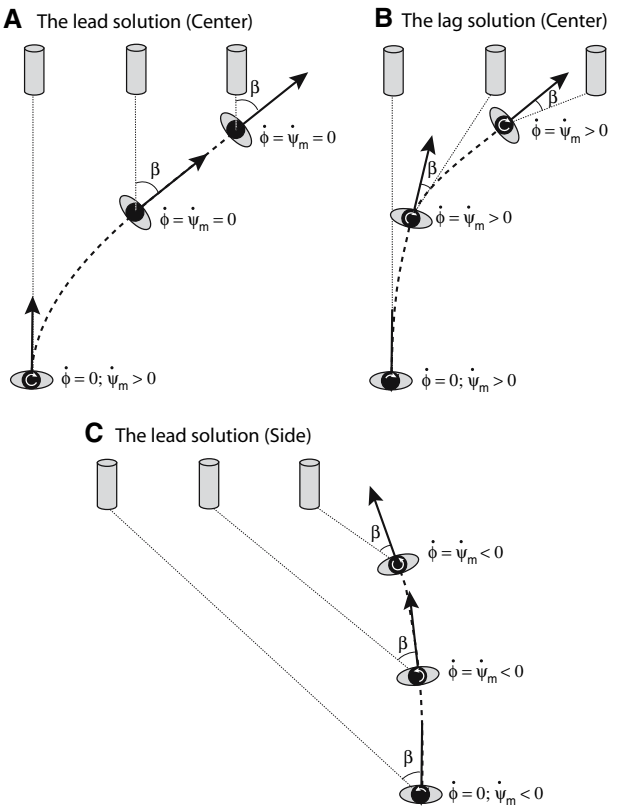

Fig. 6 Model #3: Two solutions for intercepting a moving target that null $\dot{\beta}$. **a** The "lead" solution in which the target has a constant bearing and the turning rate is zero. **b** and **c** The "lag" solution in which the (nonzero) turning rate is equal to the rate of change in bearing direction. Note that the allocentric direction of the target (ψ_m) is constant in **a**, but not in **b** and **c**

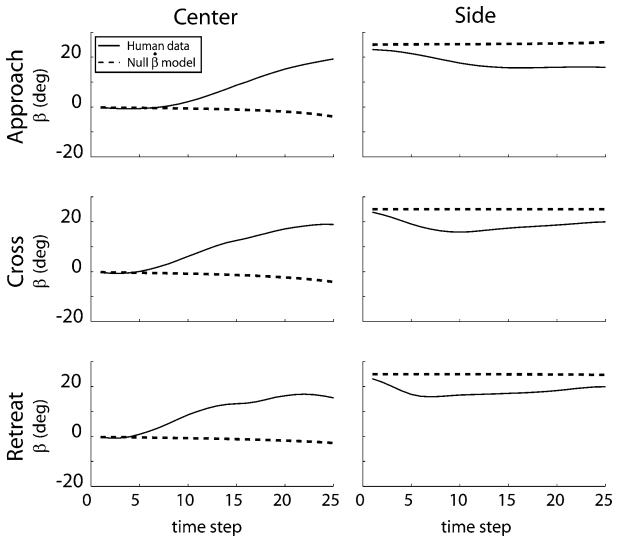

Fig. 7 Model #3: Time series of target-heading angle (β) produced by nulling $\dot{\beta}$ (*dotted lines*) compared to human data (*solid lines*)

Fig. 7, which shows the time series of the target-heading angle (β) for the human data (solid lines) and the null $\dot{\beta}$ model (dotted lines). When the target appears off to the side and moves inward, the agent leads the target like human participants (although by a greater angle). However, when the target appears in the center position and moves to the side, the agent lags behind the target. The parameters used for these simulations were $b = 1.0\ \mathrm{s}^{-1}$, $k_m = 10\ \mathrm{m}^{-1}\ \mathrm{s}^{-1}$, and $c_1 = 1.0$. These parameters were arrived at by setting c_1 to its default value (1.0), and then varying b and k_m to find a combination that yields successful interception across all six initial conditions. As long as k_m is large enough to overcome damping, the same basic behavior results from a wide range of parameter values.

To illustrate why the agent lags behind the target in the Center condition, consider how the damping and stiffness terms in Eq. 4 influence the agent's angular acceleration at different points in time. At the first time step in Fig. 6b (Center condition), the agent is moving forward along a straight path ($\dot{\phi} = 0$), and the target is moving to the right ($\dot{\psi}_m > 0$). Ignoring the distance term, the stiffness component $-k_m(\dot{\phi} - \dot{\psi}_m)$ will be positive, resulting in a clockwise angular acceleration that is opposed by the damping term $(-b\dot{\phi})$. As long as k_m is sufficiently large to overcome the damping, then the agent's turning rate $\dot{\phi}$ will eventually approach $\dot{\psi}_m$, at which point $-k_m(\dot{\phi} - \dot{\psi}_m)$ will be close to zero. At this moment (corresponding to the second time step in Fig. 6b), the agent is close to nulling $\dot{\beta}$ by turning at approximately the same rate that the bearing of the target is changing; that is $\dot{\phi} \approx \dot{\psi}_m > 0$. Because

$-k_m(\dot{\phi} - \dot{\psi}_m) \approx 0$, the clockwise acceleration from the stiffness term is weak and is opposed by the damping term $(-b\dot{\phi})$, which accelerates the agent in the counterclockwise direction. Thus, once the agent is turning at the same rate that the target's bearing is changing, nothing acts to further accelerate the agent in the clockwise direction, so the agent settles onto a lag solution.

A similar sequence of events unfolds in the Side condition, as illustrated in Fig. 6c. However, this situation yields the lead solution because the agent's heading is in front of the target at the moment that its turning rate matches the rate of change in the bearing direction. Again, the agent is initially moving forward along a straight path $(\dot{\phi} = 0)$. As long as the target appears far enough off to the side, then $\dot{\psi}_m$ will be less than zero due to the agent's forward motion. Ignoring the distance term, the stiffness term $-k_m(\dot{\phi} - \dot{\psi}_m)$ will be less than zero, resulting in a counterclockwise angular acceleration. The stiffness term continues to produce counterclockwise rotation until $\dot{\phi} = \dot{\psi}_m$; that is, until the agent is turning at the same rate that the bearing of the target is changing. At this point, corresponding to the second and third time steps in Fig. 6c, neither the stiffness nor the damping produces acceleration in the counterclockwise direction. So the agent settles onto a lead solution.

In sum, nulling $\dot{\beta}$ fails to capture the human interception strategy. It produces a lag solution with continuously curved paths under conditions in which humans clearly adopt the lead solution with linear paths to the target.

Model #4: Constant bearing (null $\dot{\psi}_m$ or null $\dot{\beta} - \dot{\phi}$)

A fourth possibility is the constant bearing strategy, which nulls change in the target's bearing direction. There are two formally equivalent formulations of Model #4. The first version nulls change in the bearing direction $(\dot{\psi}_m)$:

$$\ddot{\phi} = -b\dot{\phi} + k_m\dot{\psi}_m(d_m + c_1) \tag{5a}$$

This version requires a visible external reference frame relative to which the change in target direction can be perceived, which could be provided by a fixed background or distant landmarks. Otherwise, the visual direction of the target would be affected by observer rotation.

An equivalent version of the model that does not require an external reference frame can be derived by replacing $-\dot{\psi}_m$ with $\dot{\beta} - \dot{\phi}$, which follows from the definition of the change in target-heading angle $(\dot{\beta} = \dot{\phi} - \dot{\psi}_m$; see Fig. 1a). Thus,

$$\ddot{\phi} = -b\dot{\phi} - k_m(\dot{\beta} - \dot{\phi})(d_m + c_1). \tag{5b}$$

This alternative works by nulling change in the target-heading angle $(\dot{\beta})$ while factoring out the influence of turning rate $(\dot{\phi})$, thereby compensating for observer rotation. There are two ways of thinking about the informational basis of Eq. 5b. First, information for the changing angle $\dot{\beta}$ is provided by the visual direction of the target relative to the heading direction, which could be determined from optic flow or podokinetic information, whereas information about the changing heading $\dot{\phi}$ is potentially available from optic flow, podokinetic, and vestibular sources. Second, if one assumes that the locomotor axis is aligned with the body midline (ruling out a ''crabbing'' gait), then $\dot{\beta}$ is equivalent to the changing egocentric direction of the target, and $\dot{\phi}$ is again equivalent to the body's rotation rate. The equivalence of these two interpretations (Eq. 5a, b) is illustrated in Fig. 6a. When the agent follows a straight interception path to the target, both the change in bearing direction $(\dot{\psi}_m)$, and the difference between the change in target-heading angle and the agent's turning rate $(\dot{\beta} - \dot{\phi})$ are zero.

To illustrate why Model #4 eliminates the lag solution, compare Eq. 5b with Model #3. The stiffness components of these models are $-k_m\ (\dot{\beta} - \dot{\phi})$ and $-k_m(\dot{\beta})$, respectively. The critical difference between the two models, and the reason that Model #4 eliminates the lag solution, is that it factors out the influence of turning rate $(\dot{\phi})$. Referring to Fig. 6, consider again what happens in the Center condition at that critical moment when the agent is nulling $\dot{\beta}$ by turning at the same rate that the target bearing is changing. Recall that angular acceleration in Model #3 drops to zero at this point because $\dot{\beta}$ equals zero, resulting in the path shown in Fig. 6b. By comparison, angular acceleration in Model #4 is positive at this moment because the agent is rotating at the same rate that the bearing direction is changing. So, although $\dot{\beta} = 0, \dot{\phi} > 0$ and hence the agent's angular acceleration is $-b\dot{\phi} - k_m(-\dot{\phi})(d_m + c_1) = [k_m(d_m + c_1) - b]\dot{\phi}$ (see Eq. 5b). As long as $k_m\ (d_m + c_1)$ is large enough compared to b, the agent's angular acceleration will be positive, turning the agent clockwise to a positive bearing angle, resulting in the path shown in Fig. 6a.

Simulations of Eq. 5a, b capture the basic pattern of human behavior shown in Fig. 2, specifically an initial turn onto a straight path toward the target. The target-heading angle evolves from its initial value toward the predicted interception angle, similar to the human data

in Fig. 3. Thus, the principle of nulling $\dot{\psi}_m$ (or equivalently, nulling $\dot{\beta}$ while factoring out the influence of $\dot{\phi}$) generates the basic steering dynamics of interception. However, the simulations were missing the slight S-shaped bend that occurs in the human paths in the Side condition.

Latency

We hypothesized that the S-bend in the Side condition could be due to a latency to detect and respond to target motion. If the target is initially perceived as stationary, participants would first turn toward it; once the target's motion was detected, they would then turn back ahead of it. In the model, distal target motion affects $\dot{\psi}_m$ (i.e., target bearing direction). However, $\dot{\psi}_m$ also depends on the motion of the observer. So, we split $\dot{\psi}_m$ into a component due to observer movement and a component due to target motion itself, $\dot{\psi}_m = \dot{\psi}_{m-\text{obs}} + \dot{\psi}_{m-\text{tar}}$. The latency of target motion detection was then incorporated into the model by weighting $\dot{\psi}_{m-\text{tar}}$ by a coefficient s, which varies as a sigmoidal function of time

$$s = \frac{1}{1 + ne^{-mt}}. \tag{6}$$

Parameter n was set to a large value (n = 1,000) so that the sigmoidal function would increase from near zero at t = 0 to one. The slope m was set to 25 to produce a total latency of approximately 0.5 s, based on data in the literature regarding the visuo-motor delay. For example, the visuo-motor delay for the onset of an arm movement to punch a falling ball has been estimated at about 0.25 s (Michaels et al. 2001); we double this to approximate a visual delay to detect that the target is moving and a locomotor delay to overcome the inertia of the body.

The results appear in Fig. 8. The simulated paths (dotted lines) are very close to the human paths (solid lines). In the Center condition, the target appears straight ahead so the model initially moves toward it, and then makes a smooth curve onto a relatively straight interception path. In the Side condition, the target appears 25° to one side and the path initially curves toward it slightly before doubling back to lead it. Thus, the latency to detect and respond to target motion can account for the shallow S-bend in the human data.

The time series of target-heading angle are presented in Fig. 9. The simulations (dotted black lines) also match the human data (solid black lines) quite well, including the subtle variation across conditions.

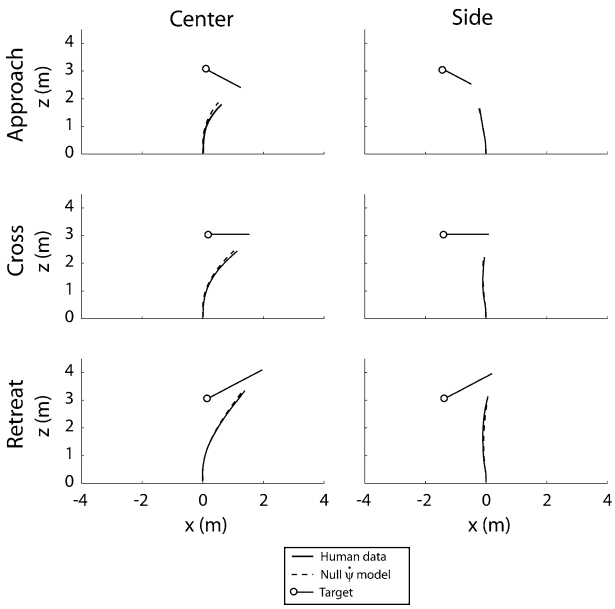

Fig. 8 Model #4: Paths produced by nulling $\dot{\beta} - \dot{\phi}$ (dotted lines) compared to human data (solid lines)

In the Center condition, the angle starts at zero, dips slightly as the moving target briefly leads the heading due to the latency, then rises to a peak. In the Side condition, the angle starts at 25° and decreases to a plateau. We fit the model to the mean time series of target-heading angle in each condition, using a least-squares procedure that minimized the error in β at every time step. c_1 was set to 1.0 by default. The fits were quite good, with a mean rmse = 2.15° and r^2 = 0.87 for parameters values of b = 7.75 s^{-1}, k_m = 6.00 m^{-1} s^{-1}, and c_1 = 1.0 m fixed across all conditions.

Background effect

In Fajen and Warren's (2004) moving target experiment, the presence of a stationary background yielded faster turns to larger target-heading angles than without a background (compare black and gray solid lines in Fig. 9). A background is known to enhance the perception of target motion (Lenoir et al. 1999b), and Fajen and Warren (2004) attributed the background effect to the visible relative motion between the target and the background. To simulate the No Background condition, we increased the latency in our interception model to 1 s by decreasing the slope of the sigmoidal function (m = 12.5). The simulations produced slower turns to smaller target-heading angles in a manner analogous to the No Background condition (gray lines in Fig. 9). Reducing the perceived target speed ($\dot{\psi}_{m-\text{tar}}$) had a similar result. Thus, the background effect can be

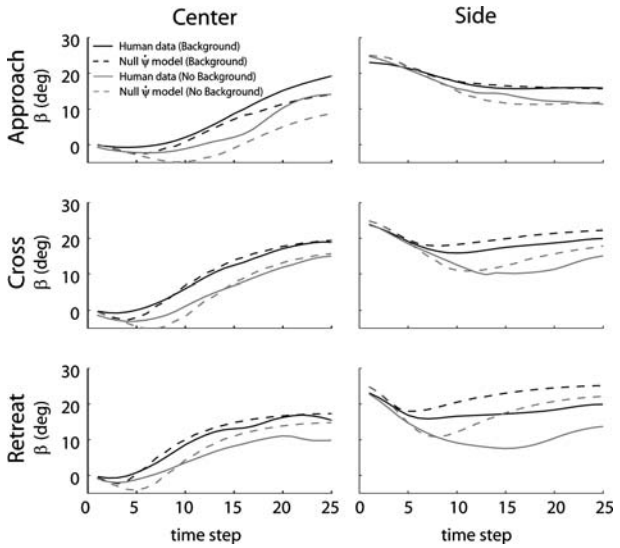

Fig. 9 Model #4: Time series of target-heading angle (β) produced by nulling $\dot{\beta} - \dot{\phi}$ (*dotted lines*) compared to human data (*solid lines*). *Black lines* correspond to Background condition; *gray lines* correspond to No Background condition

accounted for by enhancing the detection of target motion or the perceived target speed.

Distance term

To test whether the distance term in Eq. 5a, b is necessary, we simulated the model without a distance term. When the range of initial target distances is small, as it was in the experiments reported in Fajen and Warren (2004), then the model can capture human behavior without the distance term. Simulations using $b = 19.0\ s^{-1}$ and $k_m = 43.5\ s^{-1}$ yielded fits that were only slightly worse than those with the distance term (rmse = 2.48° and $r^2 = 0.79$). However, when the range of initial target distances is large, the distance term appears necessary to capture human behavior. Figure 10 shows the results of simulations using a range of initial target distances (6, 12, and 24 m). Without the distance term (gray dotted lines), the agent makes sluggish turns toward distant targets. Recall that this is due to the fact that the rate of change in target-heading angle due to the agent's movement decreases with distance. The distance term offsets this bias by weighting the influence of distant targets more heavily. Simulations with the distance term (black solid lines), using the same parameters that best fit the data from Fajen and Warren (2004) show that the agent turns more rapidly onto a straight path, keeping a constant interception angle close to the predicted $\hat{\beta}$. Assuming that human subjects also turn onto a straight path to intercept distant targets, it would seem that the distance term is needed to capture human data. Future experiments on human subjects intercepting moving targets at greater initial distances are needed to confirm this.

Other models

Finally, we note that Chardenon et al. (2004) proposed a constant target-heading angle model without a damping or a distance term for the specific case of speed adjustments on a fixed track. However, the model does not extend to steering control because a damping term is necessary to eliminate equi-angular

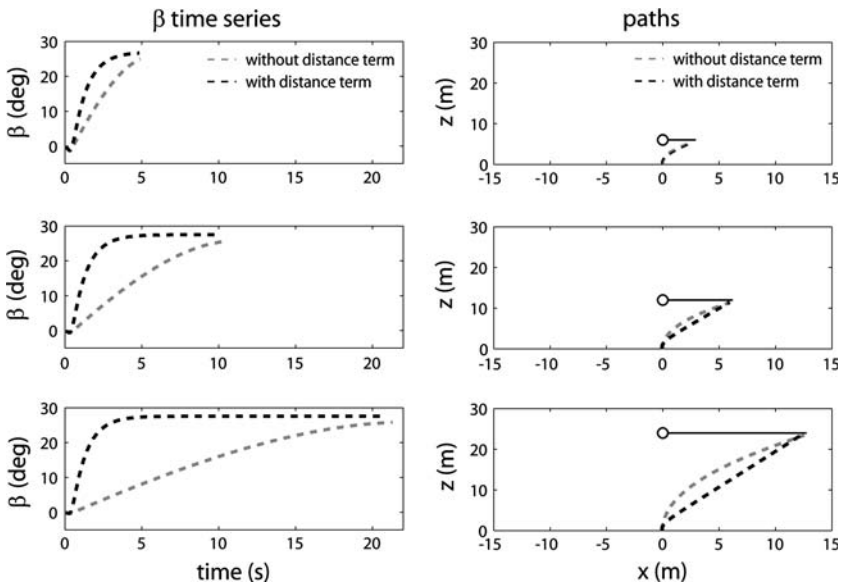

Fig. 10 Distance term: time series of target-heading angle (β) (*left column*) and paths (*right column*) produced by Model #4 with (*black lines*) and without (*gray lines*) the distance term. The rows correspond to different initial target distances (6, 12, and 24 m)

spirals about the target so we will not consider it further here.

Model robustness

To test the robustness of the constant bearing model, we ran simulations of Eq. 5a, b with different sources of variability added to the model. The effects of variability in initial conditions were tested by adding Gaussian noise to the initial lateral position and initial heading at the beginning of each simulated trial. The noise distribution for initial lateral position had a mean of zero and a standard deviation of 0.25 m (less variability) or 1.50 m (more variability). For initial heading, the noise distribution had a mean of zero and a standard deviation of 10 or 45°. The effects of perceptual error and parameter variability were simulated by adding Gaussian noise to each parameter (b, k_m, c_1) and perceptual variable ($\dot{\psi}_m$ and d_m). Specifically, each variable was multiplied by a different constant chosen from a Gaussian distribution with a mean of 1.0 and a standard deviation of 0.1 or 0.25, and new constants were randomly selected on each simulated trial. The dependent measure was the percentage of trials on which the simulated agent successfully intercepted the target. Successful trials were subdivided into ''lead'' trials, in which agent intercepted the target by turning ahead of it such that $\beta > 0$, and ''lag'' trials, in which the agent reached the target by lagging behind such that $\beta < 0$. All six conditions (two initial target locations by three target trajectories) were used in the simulations.

The results, based on 6,000 simulated trials (1,000 per initial condition) for each test, are summarized in Table 1. The model proved to be extremely robust to variability in initial conditions, successfully reaching the target along a lead interception path on 100% of the trials when both initial position and heading were varied with standard deviations of 0.25 m and 10°, respectively. Even when the standard deviation of initial position was 1.50 m and the standard deviation in heading was 45°, the model still successfully reached the target along a lead path 94.6% of the time. The model was also quite robust to variability in parameters and perceptual variables. When 10% variability was added to all three parameters or both perceptual variables, the model still successfully reached the target on 97.1 and 96.2% of the trials, respectively. When the standard deviation was increased to 0.25, the overall percentage of successful lead interceptions was still quite high, but there was an increase in the percentage of lag trials and misses.

Table 1 Results of simulations with variability

Variable or parameter	Noise level	Each trial type (%)		
		Lead	Lag	Miss
Initial x-position (cm)	25	100.0	0.0	0.0
	150	98.6	0.2	1.2
Initial heading (°)	10	100.0	0.0	0.0
	45	97.3	2.3	0.5
Both initial conditions	25/10	100.0	0.0	0.0
	150/45	94.6	2.5	2.9
b	0.10	99.5	0.5	0
	0.25	94.8	5.2	0.0
kg	0.10	98.4	1.6	0.0
	0.25	91.2	7.6	1.3
c_1	0.10	100.0	0.0	0.0
	0.25	97.5	2.5	0.0
All parameters	0.10	97.1	2.9	0.0
	0.25	88.7	9.2	2.1
$\dot{\psi}$	0.10	98.7	1.3	0.0
	0.25	91.2	7.7	1.1
Target distance	0.10	97.6	2.4	0.0
	0.25	90.7	8.6	0.8
Both perceptual variables	0.10	96.2	3.8	0.0
	0.25	85.9	10.7	3.4

One or two strategies for stationary and moving targets?

In the last set of simulations, we investigated the question of whether there are distinct strategies for steering to a stationary target and intercepting a moving target, or one unified strategy for both. Our results show that a model with two separate components, one for stationary targets that nulls the target-heading angle β (Eq. 1) and a constant bearing strategy for moving targets that nulls $-\dot{\psi}_m = \dot{\beta} - \dot{\phi}$ (Eq. 5a, b), fits the human data quite accurately. But it is also possible that a single component might account for behavior with both stationary and moving targets.

We first considered whether the stationary target model that nulls β (Model #1) might be able to account for the behavior of humans intercepting moving targets. However, it is clear that Model #1 implements a pursuit strategy that generates smoothly curved paths to a moving target and converges on a target-heading angle of zero. Our simulations of Eq. 1 confirmed this (Figs. 4, 5), and illustrate the differences between the pursuit strategy generated by a null β model and the interception strategy adopted by humans. Thus, the stationary target component cannot be applied to moving targets.

Another possible approach is Model #2, which computes the required interception angle $\hat{\beta}$ (Eq. 3). In the simulations with moving targets reported above, we showed that this model yields paths that closely match those produced by human subjects. Because Model #2

reduces to Model #1 when the target is not moving ($v_{t,m} = 0$, so $\hat{\dot{\beta}} = 0$), this model works for both stationary and moving targets. The $\hat{\dot{\beta}}$ model thus offers a single unified strategy for both stationary and moving targets, but at the price of explicitly computing the interception angle. It presumes that distal target velocity and self-motion speed can be accurately perceived, but a small error in these values can yield a large error in the interception angle, so the model is not robust. We conclude that the $\hat{\dot{\beta}}$ model is not a viable strategy.

A third possibility is that Model #3, which nulls change in the target-heading angle $\dot{\beta}$, might also apply to the case of a stationary target. The strategy was originally proposed by Llewellyn (1971), who observed that one could steer toward a stationary goal by canceling target drift in the field of view. This is equivalent to nulling $\dot{\beta}$, on the assumption that the observer is not rotating. However, if the observer can turn as well as translate, nulling $\dot{\beta}$ can also generate equi-angular spiral paths to a stationary goal (Rushton et al. 2002). Wilkie and Wann (2003, 2005) formalized a version of this strategy for stationary targets that includes damping and stiffness terms (but no distance term), and acts to null three variables: change in the visual direction of the target with respect to the locomotor axis (VD), extraretinal information for change in the gaze angle of the target with respect to the locomotor axis (ER), and the rotary retinal flow about the target (RF). The first two variables are equivalent to $\dot{\beta}$, while the third is proportional to β. Thus, in the absence of retinal flow, their model is equivalent to canceling target drift or nulling $\dot{\beta}$.

To explore this strategy with stationary targets, we formalized the model as in Eq 4, without the distance term

$$\ddot{\phi} = -b\dot{\phi} - k_g(\dot{\phi} - \dot{\psi}_g) \tag{7}$$

We have already demonstrated that this model (with or without the distance term) fails to capture moving target interception because it produces the lag solution for many initial conditions. For stationary targets, Eq. 7 successfully guides the agent to the goal, but it produces spiral paths that also differ from the human data. Initially, the agent turns toward the stationary goal. At some point before the target-heading angle reaches zero, the agent's turning rate ($\dot{\phi}$) equals the rate of change in the bearing direction of the target ($\dot{\psi}_g$), so the stiffness term becomes zero. Once this occurs, the model cannot accelerate further and becomes trapped at $\dot{\beta} = \left(\dot{\phi} - \dot{\psi}_g\right) = 0$ with the target-heading angle at a constant non-zero value ($\beta \neq 0$),

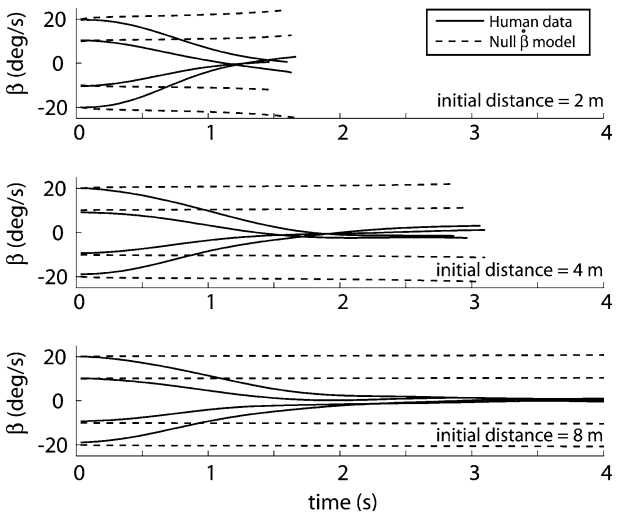

Fig. 11 Model #3: with a stationary target:time series of target-heading angle (β) produced by nulling $\dot{\beta}$ with a stationary target (same as Wilkie and Wann 2003 model; *dotted lines*) compared to human data from Fajen and Warren (2003) (*solid lines*). Initial heading angle was ±10° and ±20°, and initial distance was 2, 4, or 8 m

and the agent follows a spiral path to the goal. Figure 11 shows the β time series resulting from simulations of Eq. 7 (dotted lines) compared to the data from Fajen and Warren (2003) of human subjects (solid lines) walking to stationary goals at different initial angles and distances. Notice that Eq. 7 yields a constant non-zero value of β, whereas β converges to zero in the human data. Thus, the null $\dot{\beta}$ model fails to capture human behavior with both stationary and moving targets.

The final candidate for a unified model is Model #4, the constant bearing strategy that nulls $-\dot{\psi}_m$ (Eq. 5a, b). Having already established that this model successfully reproduces the behavior of human subjects intercepting moving targets, we considered whether Eq. 5a, b might also work for stationary targets. Figure 12 shows the results of simulations of Eq. 5a, b using stationary targets at the same initial angles and distances used in Fajen and Warren (2003).[5] The fit was quite good (rmse = 1.06° and $r^2 = 0.98$), indicating that Eq. 5a, b can also capture the behavior of human subjects steering to stationary targets. However, the parameters used in these simulations (b = 3.0 s^{-1}, k_g = 2.00 m^{-1} s^{-1}, and c_1 = 4.0 m) were somewhat different from those that best fit the moving target data. Thus, the constant

[5] For simulations of Eq. 5a, b with stationary targets, the simulated speed of the agent was changed to 1.0 to match the speed that was used in simulations of Fajen and Warren's (2003) stationary target model.

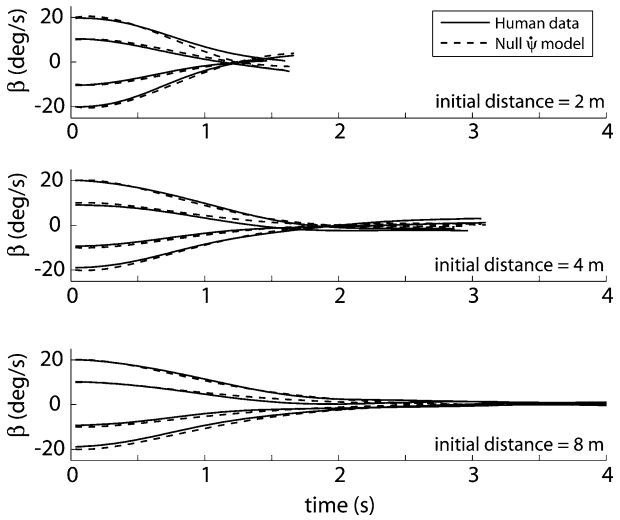

Fig. 12 Model #4 with a stationary target:time series of target-heading angle (β) produced by nulling $\dot{\beta} - \dot{\phi}$ with a stationary target (*dotted lines*) compared to human data from Fajen and Warren (2003) (*solid lines*). Initial heading angle was ±10° and ±20°, and initial distance was 2, 4, or 8 m

bearing model works for both stationary and moving targets, but with a different set of parameter values.

Other evidence indicates that different information is used to guide walking to stationary and moving targets. As reviewed in the introduction, participants rely on both optic flow and egocentric direction to walk to a stationary goal, but appear to rely solely on egocentric direction to intercept a moving target. These results are consistent with two distinct strategies: a stationary goal strategy that nulls the target-heading angle (Model #1), and a target interception strategy that nulls change in the bearing direction (Model #4). Switching between strategies would presumably depend on a threshold for detecting and responding to target motion, consistent with Lenoir et al.'s (2002) finding that interception adjustments are initiated at a critical rate of change in the bearing direction (3–5°/s).

Discussion

A straightforward extension of our steering dynamics model for stationary goals successfully accounts for human interception of moving targets (Model #4). The model nulls change in the target's bearing direction ($\dot{\psi}_m$), which is formally equivalent to nulling change in target-heading angle while factoring out the turning rate ($\dot{\beta} - \dot{\phi}$). It generates turns onto a straight interception path that leads the target, and is thus sufficient to reproduce the essential form of human paths as well as the transients observed in the time-course of the target-heading angle.

With refinement, the model also accounts for two puzzling aspects of the human data. First, the subtle S-bend in the path in some conditions was reproduced by adding a constant for the latency to detect and respond to target motion. Second, the influence of a visible background on steering behavior can also be accounted for by its influence on the detection of target motion. The results demonstrate how a constant bearing strategy could underlie interception, yet the observed behavior be dominated by transient dynamics, particularly at short target distances.

Model comparisons

We compared four possible models to determine how well they could to account for human data on target interception. Model #1 acts to null the target-heading angle β and was developed to model steering to a stationary goal. With moving targets it corresponds to a pursuit strategy that heads toward the target's current direction and generates continuously curved paths, contrary to the human interception strategy. Model #2 computes the required interception angle $\hat{\beta}$ from perceived distal target velocity and perceived locomotor speed. However, it is not robust to small amounts of error or noise in the perceived target velocity. Model #3 nulls change in the target-heading angle. Although under some initial conditions this model displays one solution that leads the target and generates human-like interception paths, under other conditions it exhibits a second solution that lags the target and generates spiral paths, which are not observed in the human data. The best fit was achieved with Model #4, which nulls change in the target's bearing direction, generating interception paths that capture the human data (rmse = 2.15°, $r^2 = 0.87$). It eliminates the lag solution, is robust to noise in perceptual variables and parameters, and is plausibly based on available information.

Information

Having identified a control strategy that accounts for human interception, we return to the question of the information that might be used to guide it. One version of Model #4 (Eq. 5a) proposes that the agent nulls change in the bearing direction of the target ($\dot{\psi}_m$), where ψ_m is the visual direction of the target in an allocentric reference frame (see Fig. 1a). This requires a visible external reference such as a fixed background or distant landmark relative to which the change in

target direction can be perceived, independent of observer rotation, analogous to the dragonfly's use of the horizon (Olberg et al. 2000). However, Fajen and Warren (2004) found that interception behavior was similar with and without a visible background (textured floor, walls, and ceiling), as well as when motion was added to the background. These results indicate that a visible reference frame is neither necessary nor used when available, casting doubt on the first version of the constant bearing model.

The second version (Eq. 5b) proposes that the agent eliminates the effects of rotation by factoring out observer turning rate ($\dot{\phi}$) from the change in target-heading angle ($\dot{\beta}$). First, $\dot{\beta}$ could be determined with respect to the heading specified by optic flow or the locomotor axis specified by proprioceptive and motor information; $\dot{\phi}$ could be independently determined from the rotational component of optic flow, or from vestibular or podokinetic information. However, recent evidence indicates that vestibular information does not contribute to estimates of locomotor rotation (Crowell et al. 1998; Wilkie and Wann 2005), and that heading from optic flow does not contribute to target interception (Fajen and Warren 2004). In contrast, proprioception appears to play a role in interception during treadmill walking (Bastin et al. 2006). This leads to the conclusion that for moving targets, change in the target-heading angle $\dot{\beta}$ is determined from proprioception about gaze angle with respect to the locomotor axis, and change in heading direction $\dot{\phi}$ is determined from podokinetic information.

One strategy or two?

The present study raises an interesting question about the organization of locomotor behavior: do people switch between two distinct strategies for stationary and moving targets, or do they use one unified strategy? Our simulations show that Model #1 fails to generalize from stationary to moving targets, while Model #3 fails to generalize in reverse, and Model #2 is not sufficiently robust in either case. Interestingly, Model #4, the constant bearing strategy, successfully generalizes from moving to stationary targets, although it requires a different set of parameter values. But other evidence indicates that humans make use of different information in the two cases, relying on optic flow to steer toward a stationary goal, but not to intercept moving targets (Fajen and Warren 2004). The computational and empirical evidence thus coheres around two distinct strategies: one for steering to stationary goals that nulls the target-heading angle (Model #1), and one for intercepting moving targets that nulls change in the bearing direction (Model #4).

Neural implications

The present findings have several implications for our understanding of the multisensory cortical networks involved in self-motion and locomotor control. First, the control of steering to stationary targets appears to rely on information about target-heading angle based on optic flow and egocentric direction. This is consistent with recent findings that human areas STP and SPL respond to heading with respect to landmarks, and heading error during steering (Vaina and Soloviev 2004; Field et al. 2006). In contrast, the present results imply that the interception of moving targets is controlled by the bearing direction of the target in allocentric space. This appears to be derived from proprioceptive and motor information about the changing target-heading angle ($\dot{\beta}$) and the changing locomotor axis ($\dot{\phi}$). These results indicate the importance of investigating the neural basis for proprioceptive information from the neck and trunk, and podokinetic information from the legs and feet, and how it is integrated in cortical self-motion networks.

Investigation of the brain areas that are active during locomotor interception could provide important clues about how the change in bearing direction is estimated. It is generally accepted that areas of the brain associated with the coding of objects in egocentric reference frames are distinct from those associated with allocentric coding. Whereas egocentric reference frames are associated with the parietal–frontal cortex, allocentric reference frames are associated with the hippocampal–parahippocampal region and retrosplenial cortex (e.g., Committeri et al. 2004; Galati et al. 2000). If the change in bearing direction is derived from the changing target-heading angle and the changing locomotor axis, then we would expect locomotor interception to elicit activity in areas of the brain that code objects in egocentric but not allocentric reference frames. This would be consistent with the view that egocentric reference frames are primarily used for visual-motor tasks. If, on the other hand, this information is used to update the target's bearing direction in an allocentric reference frame, then activity in allocentric brain areas may be expected.

Finally, the steering dynamics model implies that control laws map heading error and bearing direction into locomotor commands for turning. This suggests further investigation into how such sensorimotor transformations might be implemented in areas such as PEc and M1.

New predictions

The basic principle of the constant bearing model is that the agent continuously nulls change in the current target bearing, yielding what appears to be anticipatory behavior without predicting the target's trajectory in 3D space. The model thus makes some counter-intuitive predictions. First, if the target accelerates, it predicts that humans will not anticipate the target's motion and adopt a straight interception path, but will trace out a continuously curved path. Second, if the target travels on a circular trajectory, the model again predicts that humans will chase after the target on a continuously curved trajectory, rather than taking a short-cut across the circle. Finally, if the target travels on an irregular trajectory, the constant bearing model predicts different paths from the constant target-heading angle model. Current research is investigating these predictions.

In conclusion, the present results characterize the behavioral dynamics of steering to moving as well as stationary targets in human locomotion. Our original model showed how steering and obstacle avoidance emerge from a system that tracks locally specified attractors as they evolve with locomotion through a static environment. The present model extends this principle to interactions with a moving target. It captures the intuition that people intercept moving targets, like football's open-field tackle, by maintaining a constant bearing direction, while at the same time accounting for the transient dynamics of actual behavior. The next step in this research will apply the constant bearing principle to avoiding moving obstacles. The long-term aim of this research program is to predict human paths in arbitrarily complex environments by additively combining these elementary components. This work extends the dynamical systems approach to human movement (Kelso 1995; Kugler and Turvey 1987) from rhythmic laboratory tasks to complex behavior with non-stationary dynamics, in which the layout of attractors depends on the interaction with the environment.

Acknowledgments This research was supported by the National Eye Institute (EY10923), National Institute of Mental Health (K02 MH01353) and the National Science Foundation (NSF 9720327).

Appendix

The appendix describes the methods used in the human experiments and the model simulations.

Human data

The human data were collected in the Virtual Environment Navigation Lab at Brown University (Spiro 2001; for details, see Fajen and Warren 2004). Eight volunteers walked in a 12×12 m^2 area while wearing a head mounted display (Kaiser Proview 80, field of view 60° H × 40° V). Head position and orientation were recorded with an ultrasound/inertial tracking system (Intersense IS-900) at 60 Hz. The virtual environment was generated on a graphics workstation (SGI Onyx2 IR) and presented stereoscopically at 60 frames/s, with a latency of approximately 50–70 ms (3–4 frames). The target was a marble-textured cylinder (2.5 m tall, 0.1 m radius) that moved horizontally at a speed of 0.6 m/s. After the participant walked 1 m in a specified direction, the target appeared at a distance of 3 m along the z axis, either directly in front of the participant at 0° (Center condition) or 25° to the left of the participant's initial heading (Side condition). It either moved rightward perpendicular to the initial heading (Cross condition), approached at an angle of 30° from the perpendicular (approach), or retreated at an angle of 30° (retreat). These conditions were mirrored left/right and the data collapsed. In the No Background condition, the target moved in empty black space; in the Background condition, the target moved in a room with random-textured floor, walls, and ceiling. There were 10 trials in each condition, blocked by Background and randomized within blocks. Head position in x and z was filtered (zero-lag, 0.6 Hz cutoff) and the direction of motion (ϕ) was computed for each pair of frames. Because the filter compresses data points near the end of the time series, there is an artifactual drop in speed and heading angle. So we truncated the last 500 ms of the filtered time series to eliminate these effects. The time series of target-heading angle (β) for each trial was normalized to a length of 25 data points by subsampling, and the mean time series was computed in each condition.

Model simulations

The method used to simulate each model will be illustrated using model #4 (null -$\dot{\psi}_m$; Eq. 5a, b). The agent's angular acceleration is a function of the agent's rate of rotation ($\dot{\phi}$), the change in allocentric direction of the target ($\dot{\psi}_m$), and the target distance $d_m.\dot{\psi}_m$ can be expressed as a function of the agent's position (x_a, z_a) and speed ($v_{x,a}$, $v_{z,a}$), and the target's position (x_m, z_m) and speed ($v_{x,m}$, $v_{z,m}$)

$$\dot{\psi}_m = \left[\frac{(z_m - z_a)(v_{x,m} - v_{x,a}) - (x_m - x_a)(v_{z,m} - v_{z,a})}{(x_m - x_a)^2 + (z_m - z_a)^2}\right]. \quad (8)$$

Likewise, d_m can be expressed as a function of the agent's position and the target's position

$$d_m = \left[(x_m - x_a)^2 + (z_m - z_a)^2\right]^{1/2}. \quad (9)$$

Locomotion toward a moving target is thus represented as a 6D system, for to predict the agent's future position we need to know its current heading ($y_1 = \varphi$), turning rate ($y_2 = \dot{\phi}$), and position ($y_3 = x_a$, $y_4 = z_a$), as well as the position of the target ($y_5 = x_g$; $y_6 = z_m$) assuming that agent speed (v_a), target speed (v_m), and target direction of motion (γ) are given. Written as a system of first-order differential equations, the full constant bearing model is given by

$$\begin{aligned}
\dot{y}_1 &= \dot{\phi} \\
\dot{y}_2 &= \ddot{y}_1 = \ddot{\phi} = -by_2 + k_m\dot{\psi}_m(d_m + c_1) \\
\dot{y}_3 &= \dot{x} = v_a \sin y_1 \\
\dot{y}_4 &= \dot{z} = v_a \cos y_1 \\
\dot{y}_5 &= \dot{x}_g = v_m \cos\gamma \\
\dot{y}_6 &= \dot{z}_g = v_m \sin\gamma
\end{aligned} \quad (10)$$

simulations of Eq. 5a, b (as well as the set of equations corresponding to the other models) were performed in Matlab, using the ode45 integration routine. The model speed was constant at 1.29 m/s, equal to the mean maximum human walking speed during a trial. A run was terminated when the model came within 15 cm of the target, to prevent the target-heading angle from blowing up due to small positional errors near the target. We fit the model to the mean time series of target-heading angle in each condition by searching iteratively for the parameter values that minimized the error in β at each time step across all conditions, using a least-squares criterion. Goodness-of-fit was measured by calculating the rmse between the model β time series and the mean human β time series. We also report the r^2 based on a linear regression of the model and human β time series.

References

Bastin J, Calvin S, Montagne G (2006) Muscular proprioception contributes to the control of interceptive actions. J Exp Psychol Hum Percep Perf 32:964–972

Chapman S (1968) Catching a baseball. Am J Phys 53:849–855

Chardenon A, Montagne G, Buekers MJ, Laurent M (2002) The visual control of ball interception during human locomotion. Neurosci Lett 334:13–16

Chardenon A, Montagne G, Laurent M, Bootsma RJ (2004) The perceptual control of goal-directed locomotion: a common control architecture for interception and navigation? Exp Brain Res 158:100–108

Chardenon A, Montagne G, Laurent M, Bootsma RJ (2005) A robust solution for dealing with environmental changes in intercepting moving balls. J Mot Behav 37:52–64

Committeri G, Galati G, Paradis A, Pizzamiglio L, Berthoz A, Li Bihan D (2004) Reference frames for spatial cognition: different brain areas are involved in viewer-, object-, and landmark-centered judgments about object location. J Cogn Neurosci 16:1517–1535

Crowell JA, Banks MS, Shenoy KV, Andersen RA (1998) Visual self-motion perception during head turns. Nature Neurosci 1:732–737

Cutting JE, Vishton PM, Braren PA (1995) How we avoid collisions with stationary and moving obstacles. Psychol Rev 102:627–651

Duffy CJ (2004) The cortical analysis of optic flow. In: Chalupa L, Werner J (eds) The visual neurosciences, vol II. MIT, Cambridge, pp 1260–1261

Fajen BR, Warren WH (2003) Behavioral dynamics of steering, obstacle avoidance, and route selection. J Exp Psychol Hum Percept Perform 29:343–362

Fajen BR, Warren WH (2004) Visual guidance of intercepting a moving target on foot. Perception 33:689–715

Fajen BR, Warren WH, Temizer S, Kaelbling LP (2003) A dynamical model of visually-guided steering, obstacle avoidance, and route selection. Int J Comp Vis 54:13–34

Fink PW, Foo P, Warren WH (in press). Obstacle avoidance during walking in real and virtual environments. ACM Trans on Appl Percep

Field DT, Wilkie RM, Wann JP (2006) Neural systems for the perception of heading and visual control of steering. (submitted)

Galati G, Lobel E, Vallar G, Berthoz A, Luigi P, Le Bihan D (2000) The neural basis of egocentric and allocentric coding of space in humans: a functional magnetic resonance study. Exp Brain Res 133:156–164

Gibson JJ (1950) Perception of the visual world. Houghton-Mifflin, Boston

Harris JM, Bonas W (2002) Optic flow and scene structure do not always contribute to the control of human walking. Vis Res 42:1619–1626

Harris MG, Carre G (2001) Is optic flow used to guide walking while wearing a displacing prism? Perception 30:811–818

Hollands MA, Patla AE, Vickers JN (2002) ''Look where you're going!'': gaze behavior associated with maintaining and changing the direction of locomotion. Exp Brain Res 143:221–250

Israel I, Warren WH (2005) Vestibular, proprioceptive, and visual influences on the perception of orientation and self-motion in humans. In: Wiener SI, Taube JS (eds) Head direction cells and the neural mechanisms of spatial orientation. MIT, Cambridge, pp 347–381

Kelso JAS (1995) Dynamic patterns: the self-organization of brain and behavior. MIT, Cambridge

Kugler PN, Turvey MT (1987) Information, natural law, and the self-assembly of rhythmic movement. Erlbaum, Hillsdale

Lenoir M, Musch E, Janssens M, Thiery E, Uyttenhove J (1999a) Intercepting moving objects during self-motion. J Mot Behav 31:55–67

Lenoir M, Savelsbergh GJ, Musch E, Thiery E, Uyttenhove J, Janssens M (1999b) Intercepting moving objects during self-motion: Effects of environmental changes. Res Q Exerc Sport 70:349–360

Lenoir M, Musch E, Thiery E, Savelsbergh GJ (2002) Rate of change of angular bearing as the relevant property in a horizontal interception task during locomotion. J Motor Behav 34:385–401

Li L, Warren WH (2002) Retinal flow is sufficient for steering during simulated rotation. Psychol Sci 13:485–491

Llewellyn KR (1971) Visual guidance of locomotion. J Exp Psychol 91:245–261

Michaels CF (2001) Information and action in timing the punch of a falling ball. Quart J Exp Psychol 54A:69–93

Morrone MC, Tosetti M, Montanaro D, Fiorentini A, Cioni G, Burr DC (2000) A cortical area that responds specifically to optic flow revealed by fMRI. Nat Neurosci 3:1322–1328

Nakayama K, Loomis JM (1974) Optical velocity patterns, velocity sensitive neurons, and space perception: a hypothesis. Perception 3:63–80

Olberg RM, Worthington AH, Venator KR (2000) Prey pursuit and interception in dragonflies. J Comp Physiol A 186:155–162

Peuskens H, Sunaert S, Dupont P, van Hecks P, Orban, GA (2001) Human brain regions involved in heading estimation. J Neurosci 21:2451–2461

Raffi M, Siegel RM (2004) Multiple cortical representations of optic flow processing. In: Vaina LM, Beardsley SA, Rushton SK (eds) Optic flow and beyond. Kluwer, Dordrecht, pp 3–22

Reichardt W, Poggio T (1976) Visual control of orientation behavior in the fly: I. A quantitative analysis. Q Rev Biophys 9:311–375

Rushton SK, Harris JM, Lloyd M, Wann JP (1998) Guidance of locomotion on foot uses perceived target location rather than optic flow. Curr Biol 8:1191–1194

Rushton SK, Wen J, Allison RS (2002) Egocentric direction and the visual guidance of robot locomotion: background, theory, and implementation. Biologically motivated computer vision. In: Proceedings: lecture notes in computer science, vol 2525, pp 576–591

Schöner G, Dose M, Engels C (1995) Dynamics of behavior: theory and applications for autonomous robot architectures. Robot Auton Syst 16:213–245

Spiro JE (2001) Going with the (virtual) flow. Nat Neurosci 4:120

Telford L, Howard IP, Ohmi M (1995) Heading judgments during active and passive self-motion. Exp Brain Res 104:502–510

Turano KA, Yu D, Hao L, Hicks JC (2005) Optic-flow and egocentric-direction strategies in walking: central vs peripheral visual field. Vis Res 45:3117–3132

Vaina LM, Soloviev S (2004) Functional neuroanatomy of heading perception in humans. In: Vaina LM, Beardsley SA, Rushton SK (eds) Optic flow and beyond. Kluwer, Dordrecht, pp 109–137

Warren WH (2004) Optic flow. In: Chalupa L, Werner J (eds) The visual neurosciences, vol II. MIT, Cambridge, pp 1247–1259

Warren WH, Kay BA, Zosh WD, Duchon AP, Sahuc S (2001) Optic flow is used to control human walking. Nat Neurosci 4:213–216

Wilkie RM, Wann JP (2002) Driving as night falls: the contribution of retinal flow and visual direction to the control of steering. Curr Biol 12:2014–2017

Wilkie R, Wann J (2003) Controlling steering and judging heading: retinal flow, visual direction, and extra-retinal information. J Exp Psychol Hum Percept Perform 29:363–378

Wilkie R, Wann J (2005) The role of visual and nonvisual information in the control of locomotion. J Exp Psychol Hum Percept Perform 31:901–911

Wood RM, Harvey MA, Young CE, Beedie A, Wilson T (2000) Weighting to go with the flow? Curr Biol 10:R545–R546

Zhang T, Heuer HW, Britten KH (2004) Parietal area VIP neuronal responses to heading stimuli are encoded in head-centered coordinates. Neuron 42:993–1001